Delft University of Technology

Continuous Hydrogenation of Carbon Dioxide to Formic Acid and Methyl Formate by a Molecular Iridium Complex Stably Heterogenized on a Covalent Triazine Framework

Corral-Pérez, Juan José; Billings, Amelia; Stoian, Dragos; Urakawa, Atsushi

Important note
To cite this publication, please use the final published version (if applicable).
Please check the document version above.

COMMUNICATION

Continuous hydrogenation of carbon dioxide to formic acid and methyl formate by a molecular iridium complex stably heterogenized on a covalent triazine framework

Juan José Corral-Pérez,[a] Amelia Billings,[a] Dragos Stoian,[b] and Atsushi Urakawa*[a],[c]

Abstract: Continuous synthesis of formic acid and methyl formate via CO_2 hydrogenation is demonstrated using a molecular iridium complex stably immobilized on a solid covalent triazine framework (CTF) under high-pressure conditions. Compared to formic acid synthesis, methyl formate synthesis is advantageous to enhance the selectivity and yield of formates under kinetically favorable high temperature conditions. Transient *in situ* vibrational spectroscopy shows that the CTF strongly interacts with CO_2 and H_2, and even activates methanol. Hence, CTF is a promising support for molecular catalysts, even under harsh supercritical and flow conditions, through its strong binding capability.

The catalytic hydrogenation of CO_2 to formic acid is not only a strategic reaction aiming at CO_2 mitigation[1] and H_2 economy where formic acid serves as a hydrogen carrier[2], but also offers an advantageous alternative over the commercial process. The industrial synthesis of formic acid involves two steps: methanol carbonylation to yield methyl formate and its subsequent hydrolysis to form formic acid. The hydrolysis is a reversible reaction with a relatively unfavorable equilibrium, which requires the use of either a large excess of one of the reactants or a basic additive.[3]

Formic acid synthesis by CO_2 hydrogenation is ideal in terms of atom economy (all atoms in the reactants are found in the desired product). In reality, the greatest hindrance to its development arises from serious thermodynamic limitations.[1] It must not be forgotten that the conversion of carbon dioxide and hydrogen into formic acid is strongly endergonic ($\Delta G°_{298K}$ = 32.9 kJ mol^{-1}).[4] However, the use of solvent allows the reaction to become exergonic, for example with $\Delta G°_{298K}$ = -4 kJ mol^{-1} in the aqueous phase.[4] Successful CO_2 hydrogenation to formic acid and high turnover numbers have been reported using polar solvents or

basic additives, to shift the reaction equilibrium in the presence of a homogeneous catalyst. Transition metal complexes containing Ru, Ir, Rh, Pd, Ni, Fe, Ti, or Mo (Ru and Ir in particular)[5], are known for moderate to excellent catalytic activities.[6] The main disadvantage of this process is the recovery and recycling of expensive and soluble catalysts, which is confirmed by a technological and economic feasibility study.[7] An obvious path towards commercialization is to decrease the operating cost by using heterogeneous catalysts and their recycling, or ideally to operate the reaction under continuous flow through a reactor where a catalyst is packed inside.

Reflecting this background, potential advantages of immobilizing molecular metal complexes on solid support material are evident by combining the characteristics of homogeneous and heterogeneous catalysts.[8] In other words, the well-defined active sites provided by the molecular complexes, in theory, enable high activity and selectivity to the desired product, whilst solid support facilitates catalyst handling and separation from reactant/product fluids. In addition, the common difficulty in establishing relationships between catalyst structure and activity in heterogeneous catalysis may be overcome by the use of precisely designed active centers.[9] The material and structure of the support are of critical importance, as it must provide moieties whereby the active metal can be stably coordinated without structural destruction under reaction conditions which are often harsh (high temperature and/or pressure).

The use of covalent triazine frameworks (CTFs) as a support has attracted increasing attention since they meet all the above-mentioned requirements.[10] Catalytic activity of iridium molecular complexes immobilized on different CTFs in CO_2 hydrogenation to formate/formic acid has been demonstrated.[11] Despite the success, the catalytic tests are performed under batch conditions, thus failing to discern if the catalytic activity arises from either a leached or heterogenized complex. Furthermore, significant challenges regarding catalyst stability especially under continuous operation, elucidation of intermediate species and accessibility of the active sites remain to be addressed, before the viability of such catalysts can be critically assessed for potential industrial applications.[10c]

In this work, a CTF derived from 2,6-dicyanopyridine (DCP, **Scheme 1**) and synthesized through ionothermal conditions[12],[13] is used to immobilize $[IrCp*Cl_2]_2$ (Cp* = η^5-pentamethylcyclopentadienyl). The successful trimerization reaction of DCP to yield the desired CTF (**Scheme 1**) is confirmed by IR (**Supporting Information, Figure S1a**). [19, 25] This CTF offers more bipyridine-based moieties per CTF ring than the

[a]   J. J. Corral-Pérez, A. Billings, Prof. A. Urakawa
      Institute of Chemical Research of Catalonia (ICIQ)
      The Barcelona Institute of Science and Technology
      Av. Països Catalans 16, 43007 Tarragona (Spain)
[b]   Dr. D. Stoian
      The Swiss - Norwegian Beamlines (SNBL)
      European Synchrotron Radiation Facility (ESRF)
      BP 220, 38043 Grenoble (France)
[c]   Prof. A. Urakawa
      Catalysis Engineering, Department of Chemical Engineering, Delft
      University of Technology, Van der Maasweg 9, 2629 HZ Delft, The
   Netherlands
      E-mail: A.Urakawa@tudelft.nl

      Supporting information for this article is given via a link at the end of
      the document

reported frameworks (based on 2-bromo-5-cyanopyridine or 5,5′-dicyano-2,2′-bipyridine) to coordinate the Ir complex.[11b, 11c] This may help to prevent Ir leaching under continuous operation due to the abundant coordination sites throughout the framework. The activity of the catalyst (Ir-CTF) is tested in the CO_2 hydrogenation to formic acid or to methyl formate under continuous operation at high-pressure (300 bar) to critically evaluate the catalyst stability, induce kinetic advantages, and shift the reaction equilibrium as this reaction is known to be highly pressure-dependent.[14] The catalyst is characterized before and after the reaction by means of IR, N_2 physisorption, XRD, ICP-OES, STEM, EDX and X-ray absorption spectroscopy (XAS) measurements. Furthermore, transient *in situ* diffuse reflectance infrared Fourier transform spectroscopy (DRIFTS) studies in combination with multivariate spectral analysis are performed to elucidate surface species formed over the CTF and Ir-CTF materials.
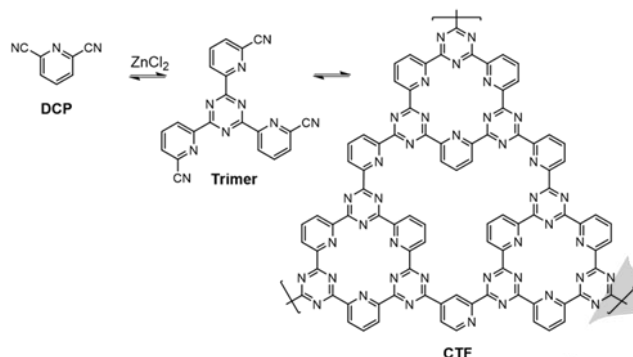
Scheme 1. Idealized schematic formation of a CTF derived from 2,6-dicyanopyridine (DCP).

The immobilization of the iridium complex on the solid CTF is performed as described in Supporting Information to yield the solid molecular catalyst depicted in **Scheme 2**. ICP-OES analysis reveals that the Ir loading of the material is 16.3 wt%. The IR features of CTF and Ir-CTF are virtually identical, confirming that the functionalization of CTF with the Ir complex does not induce changes in the framework structure (**Supporting Information, Figure S1a**). This is also confirmed by Raman spectroscopy (**Figure S1b**) and XRD (**Figure S1c**). The Raman G and D bands observed at 1580 and 1356 cm^{-1}, respectively, demonstrate that both CTF and Ir-CTF possess two-dimensional-honeycomb structure constructed from triazine and pyridine rings.[15] The broad peak in the XRD pattern at *ca.* 25° is characteristic of the graphitic layers with interlayer distance of ~3.4 Å.[15-16] The XRD pattern also indicates a predominantly amorphous structure of the materials, although a diffraction peak at *ca.* 12° appears after the immobilization of the Ir complex most likely due to the presence of chlorides in the framework.
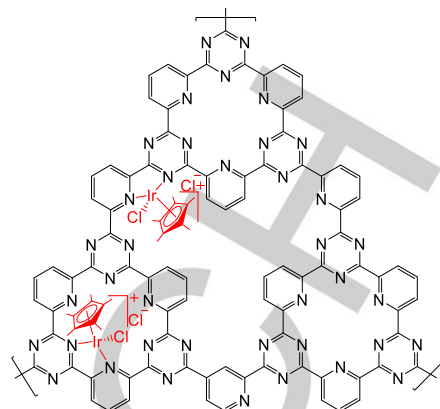
Scheme 2. Structural representation of Ir-CTF catalyst.

The porosity of these frameworks is investigated by means of N_2 physisorption. As shown in **Supporting Information, Figure S2a**, the CTF shows a type I isotherm, indicating the presence of microporosity and a limited mesoporosity. The BET surface area (S_{BET}) of 734 m^2 g^{-1} is consistent with those reported in literature for this type of CTF derived from DCP.[10c] The t-plot analysis indicates that the area attributed to micropores accounts for 97% of the total surface area. Horvath-Kawazoe pore size distribution derived from the adsorption branch of the isotherm of CTF shows that a large fraction of micropores has diameters around 0.9 nm (**Supporting Information, Figure S2b**). Interestingly, the S_{BET} of the CTF drastically decreases to 10 m^2 g^{-1} upon functionalization with the Ir complex. Such a decrease was also reported for a CTF based on 5,5′-dicyano-2,2′-bipyridine when the Ir loading was increased up to 10.6 wt%.[17] Furthermore, the N_2 adsorption-desorption isotherms of Ir-CTF are characteristic of a mesoporous material. This indicates that the Ir cationic complex and/or chlorides are largely occupying the pores of the CTF. This is further confirmed by the decrease in the total pore volume from 0.33 (CTF) to 0.016 (Ir-CTF) cm^3 g^{-1}. Consequently, the pore diameter of Ir-CTF is 3-7.5 nm (mesoporous range), as estimated by the BJH (Barrett-Joyner-Halenda) pore size distribution derived from the desorption branch of the isotherm of Ir-CTF (**Supporting Information, Figure S2c**).

Analytical techniques such as IR[16d] and EDX[18] have been used to detect the presence of the metal complex on the CTF, suggesting its direct coordination. In literature, X-ray photoelectron spectroscopy (XPS) has been widely employed to study the chemical state of the metal center, carbon and/or nitrogen.[11b, 11c, 16c, 19] However, deconvolution of XPS spectra might add uncertainty to the data.[20] In order to unambiguously determine the molecular structure of Ir-CTF, extended X-ray absorption fine structure (EXAFS) analysis of the Ir L$_3$ edge is performed in this study (**Figure 1**). According to the Fourier transforms (FT) of k^2-weighted EXAFS of the reference samples, IrCl$_3$ and Ir foil, the peaks at 1.90 and 2.55 Å can be assigned to Ir-Cl and Ir-Ir bonds, respectively.[21] This suggests that the peak observed at 1.76 Å is attributed to Ir-N bonds (1.5-2.1 Å in literature)[22] and that the Ir complex is molecularly immobilized, based on the absence of the peak attributed to metallic Ir.
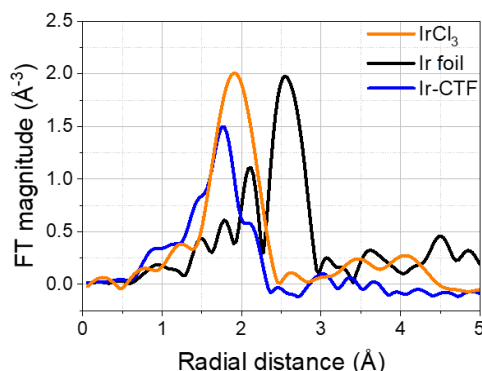
Figure 1. Fourier transforms (FT) of k^2-weighted EXAFS of $IrCl_3$, Ir foil and Ir-CTF.

The reactivity of both CTF and Ir-CTF is studied in the continuous hydrogenation of CO_2 to formates/formic acid at 300 bar. Reaction temperature above 180 °C is not investigated to avoid the formation of Ir nanoparticles. Firstly, methanol is co-fed in the reactor to produce methyl formate (MF), expectedly through the reaction between formic acid formed at the Ir active site and methanol via esterification. To our surprise, the CTF itself is slightly active in the formation of MF and the temperature has virtually no effect on its yield (**Supporting Information, Figure S3**). A blank test without methanol is performed (not shown) and no products are observed at all temperatures examined. Hence, methanol is activated over CTF, i.e. through formation of methyl and methoxy species, to yield MF. The activation of methanol over CTF is confirmed by *in situ* DRIFTS measurements, that shows methoxy species stably adsorbed over bare CTF after methanol adsorption and its subsequent desorption after thorough removal of methanol from the cell (**Supporting Information, Figure S4**). As shown in **Supporting Information, Figure S3**, the presence of Ir boosts the formation of MF at 160-180 °C. At these temperatures, CO is observed as a side-product without hindering the formation of MF. CO may be formed by the reverse water–gas shift reaction; however, it is unlikely in this low temperature range.[23] In addition, CO is not formed in the CO_2 hydrogenation in the absence of methanol (data not shown), suggesting that CO formation is due to the presence of methanol in the reaction mixture and rather to the decomposition of methyl formate and/or formic acid.

Furthermore, in order to demonstrate continuous formic acid synthesis over the Ir-CTF catalyst, water[20, 24] or triethylamine[1] is co-fed into the reactor instead of methanol to create thermodynamically favorable environment for formic acid formation (**Table 1**). At 100 °C, formic acid is selectively formed and its weight time yield (WTY) is much higher in triethylamine than in water, as expected from the stronger molecular interaction between the base and formic acid. In contrast, at 180 °C the WTY of formic acid is greater in water, likely because the dissociation of the adduct formed with the amine to formic acid and its further decomposition occurs at the temperature.[7] Generally, the overall turnover frequency (TOF) is higher at 180 °C (TOF_{total} of 7.33 and 8.94 in water and triethylamine, respectively) than at 100 °C (TOF_{total} of 0.23 and 1.61, respectively), although undesired CO

formation is prominent at 180 °C. On the other hand, when the reaction is performed in methanol, the WTY of MF is greatly enhanced at 180 °C compared to at 100 °C, while retaining high selectivity to MF (TOF_{MF} of 3.03). In this sense, MF is an interesting intermediate product to achieve fast reaction kinetics, which is favored at higher temperature, to selectivity synthesize formic acid through hydrolysis of methyl formate.[25]

Table 1. Effects of water and triethylamine (Et_3N) cofeeding and temperature on the weight time yield (WTY) of FA, MF, and CO over Ir-CTF catalyst. In brackets, TOF values are shown. For these calculations, the amount of Ir stably present during the reaction was used. Reaction conditions: 300 bar, GHSV = 14000 h^{-1}.

Reactant mixture[a]	T (ºC)	WTY_{FA} (mg_{FA} g_{Ir}^{-1} h^{-1})	WTY_{MF} (mg_{MF} g_{Ir}^{-1} h^{-1})	WTY_{CO} (mg_{CO} g_{Ir}^{-1} h^{-1})
$CO_2 + H_2$ + CH_3OH	100	-	264.5 (0.85)	-
	180	-	944.4 (3.03)	199.8 (1.37)
$CO_2 + H_2$ + H_2O	100	53.9 (0.23)	-	-
	180	44.7 (0.19)	-	1039.5 (7.14)
$CO_2 + H_2$ + Et_3N	100	385.5 (1.61)	-	-
	180	5.3 (0.02)	-	1300.0 (8.92)

[a] 4:4:1 molar ratio.

The Ir-CTF after the reaction is characterized, showing no clear indication of structural change (**Supporting Information, Figure S5**). In XRD the reflection peak at *ca.* 12° disappears and this indicates some leaching of the complex or chemical entity during the reaction (**Supporting Information, Figure S6**). The BET surface area of the spent catalyst increases to 61 m^2 g^{-1} by releasing the pore of the CTF blocked by an excess of the Ir complex. Indeed, the Ir content of the catalyst after the reaction determined by ICP-OES decreases to 7.6 wt%, confirming a certain loss of Ir during the reaction. It is important to note that despite the metal leaching, almost half of the initially loaded Ir remains in the solid framework during the reaction under the flow conditions for *ca.* 96 h at 300 bar. The presented catalytic results are obtained when the catalytic activity is stabilized after more than 48 h of stabilization under the flow of the reaction mixture. Therefore, we can safely conclude that the activity originates from the stably immobilized active Ir sites.

In order to study the changes in the electronic state and coordination environment of the Ir during the reaction, XAS measurements are performed at room temperature at Ir L_3 edge (**Supporting Information, Figure S7-S8**). Based on the absorption edge shifting towards higher energy and on the increasing white line intensity (**Supporting Information, Figure S7**), the Ir in the spent catalysts has a more oxidic character compared to the fresh catalyst. This may be due to the presence of coordinating species on Ir during the reaction, or possible oxidation of the Ir-hydride active center upon exposure to air. Both would serve as an indirect proof of the presence of a single-site Ir active center during the reaction. The EXAFS results also show

that Ir is isolated within the CTF matrix after the reaction based on the absence of the peak at 2.55 Å characteristic of Ir-Ir bonds (*vide supra*) (**Supporting Information, Figure S8**). STEM and EDX analyses further confirm the homogeneous dispersion of Ir before and after the reaction as depicted in **Figure 2** (**Supporting Information, Figure S9**).
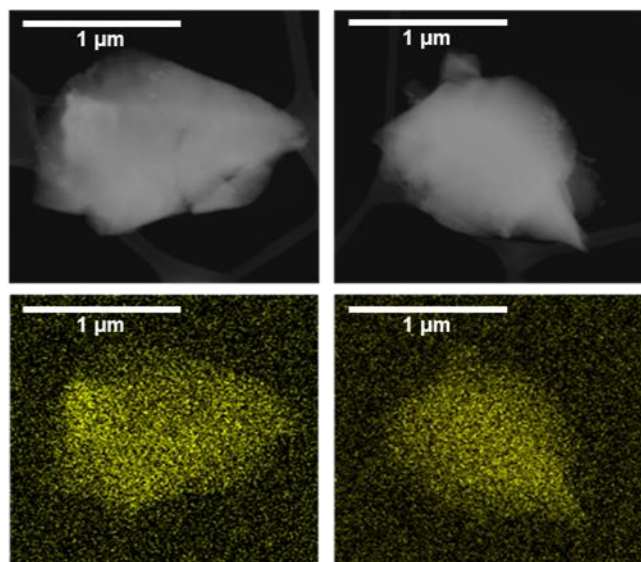

Figure 2. STEM and EDX mapping images of iridium (yellow) for Ir-CTF before (left) and after (right) the reaction.

The catalytic activity of Ir-CTF towards methyl formate and formic acid confirms the formation of formates over the catalyst surface. However, to the best of our knowledge, there is no report on the nature of the surface species formed over CTFs during CO_2 hydrogenation. In order to unravel the interaction of these frameworks with CO_2 and H_2, *in situ* DRIFTS measurements are performed with CTF and Ir-CTF in the mixture of CO_2 and H_2 at 140 °C and 5 bar. As depicted in **Figure 3**, no notable spectroscopic features are observed for CTF. On the other hand, the presence of Ir induces the formation of surface species, as indicated by the bands in the region between 1750 and 2200 cm^{-1}. The absence of bands in the v(C–H) region (2600 – 3100 cm^{-1}) implies that bidentate formates are not present over Ir-CTF. The concentration of the surfaces species is drastically increased at higher pressures (**Figure 3**), as reported for bidentate formates over silica-supported silver nanoparticles.[26] Interestingly, for both CTF and Ir-CTF, the spectral region between 2250 and 2400 cm^{-1} shows the presence of distinct spectral features which overlap with but are obviously different from the bands of gaseous CO_2. This is attributed to the excellent CO_2 adsorption capabilities of the CTF through its numerous nitrogen sites present in the framework serving as Lewis basic sites,[16a] although very little is known about the interaction between CO_2 with these nitrogen-rich materials.
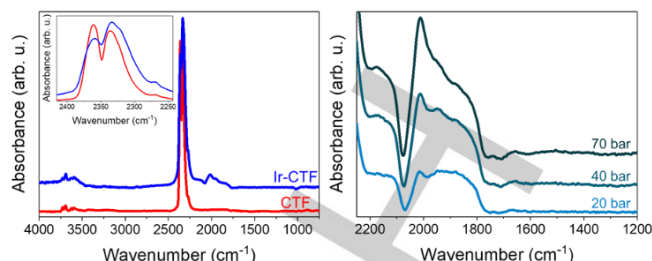

Figure 3. (Left) *In situ* DRIFT spectra of CTF and Ir-CTF upon exposure to CO_2:H_2 = 1:1 (molar ratio) at 140 °C and 5 bar. The frequency region of asymmetric CO_2 stretching vibration is enlarged for clarity. (Right) *In situ* DRIFT of Ir-CTF upon exposure to CO_2:H_2 = 1:1 (molar ratio) at 140 °C and 20, 40 and 70 bar.

To gain more precise information about the nature of CO_2 interaction with the CTF and Ir-CTF, a transient *in situ* DRIFTS study is performed by alternatingly passing pure CO_2 and Ar over CTF and Ir-CTF at 140 °C and 5 bar (**Supporting Information, Figure S10**). The results show that there are three kinetically separable species (**Figure 4**) over the CTF. The band at 2334 cm^{-1} (**Figure 4**, black) is assigned to asymmetric stretching of CO_2 adsorbed on CTF due to a clear restriction of molecular rotation. Its concentration profile indicates that the CO_2 is strongly adsorbed since it is slowly removed by Ar at the relatively high temperature. Although the spectral features of the other two species (**Figure 4**, orange and blue lines) somewhat resemble that of gaseous CO_2, their bands are highly distorted. In fact, the concentration profile of one species (**Figure 4**, blue line) follows the expected profile of CO_2 gas in the DRIFTS cell. The distortion of the spectral features may be caused by the strong electrostatic interactions between the nitrogen sites and the carbon atoms of the CO_2 molecules.[27] In case of Ir-CTF, the band of CO_2 adsorbed on CTF is also observed, but its removal is faster under Ar. This weaker interaction of CO_2 with the framework is likely caused by the decrease in the surface area when Ir is present (**Supporting Information, Figure S2**). For Ir-CTF, the two kinetically distinguishable spectra due to weakly interacting CO_2 with the material (**Figure 4**, orange and blue lines) show new spectral features in comparison to the case of CTF. Hence, the Ir complex induces different interactions with CO_2,[28] but not very strongly as suggested by the concentration profiles of these species. Furthermore, a direct interaction of CO_2 with the Ir sites is implied by the emergence of a band at 2008 cm^{-1} under CO_2 over Ir-CTF (**Supporting Information, Figure S10**), which may be attributed to η^2-C,O mode of CO_2 on the metal.[29]
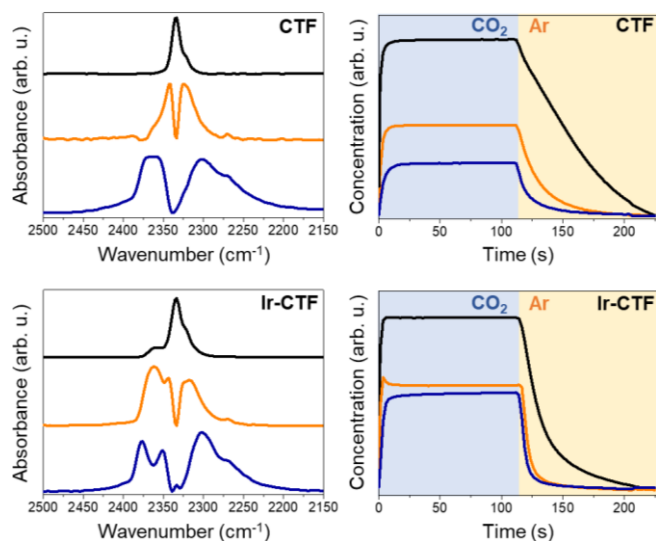
Figure 4. Components spectra and the corresponding concentration profiles obtained by multivariate spectral analysis applied on the time-resolved DRIFT spectra of CTF and Ir-CTF upon exposure to CO_2 (the first half period) and then to Ar (the second half period) at 140 ºC and 5 bar.

Figure 5. Transient DRIFTS study over CTF and Ir-CTF. Time-resolved DRIFT spectra upon exposure to H_2 or D_2 (the first half period) and then to Ar (the second half period) at 140 °C and 5 bar. The DRIFT spectra are shown in milli-absorbance unit taking the last spectrum in the Ar atmosphere as background.

The activation of CO_2 over Ir may promote the formation of formates or formic acid, provided that hydride or atomic hydrogen is present on the metal. In order to prove the presence of hydride, a transient *in situ* DRIFTS study is performed by alternatingly passing pure H_2 and Ar over Ir-CTF at 140 °C and 5 bar (**Figure 5**). Under H_2, bands at 1950, 2141 and 2264 cm⁻¹ appear together and gradually. After switching to Ar, these bands progressively decrease, thus indicating a strong interaction and a relatively high stability in Ar. These bands are not observed over bare CTF (**Figure 5**). Hence, the observed spectroscopic features point to the existence of an interaction between Ir and H_2. According to literature, these bands can be assigned to Ir-H stretching vibrations.[30] The interaction between Ir and hydrogen is further confirmed by the slight shifts of these bands in a transient study using deuterium instead of hydrogen (**Figure 5**). This small shift may indicate dominant presence of a molecular H_2 complex (Ir-H_2 or Ir-D_2 – precursor of hydride)[31] instead of hydride as transiently and reversibly formed species in response to the concentration changes of hydrogen molecules in the gas phase.[14b] After having proved that CO_2 can be activated over Ir and CTF separately, while H_2 is exclusively activated on Ir to yield hydride/H_2 species, the formation of formate or formic acid over Ir-CTF via CO_2 hydrogenation is naturally explained. The strong interaction of CO_2 with CTF would be particularly beneficial to enhance the local concentration of CO_2 near Ir. In the *in situ* DRIFT spectra of Ir-CTF upon exposure to CO_2 and H_2 (**Figure 3**), the bands attributed to the activation of CO_2 and H_2 at 1741, 1888 and 2175 cm⁻¹, which are not observed in only CO_2 (**Figure 4**) or H_2 (**Figure 5**), can be unambiguously elucidated. As mentioned above, the absence of bands in the *v*(C–H) region excludes the presence of bidentate formates (κ²-HCOO). Hence, these features indicate that monodentate formate species (κ¹-HCOO) is formed at the Ir site as well accepted for Ru-catalyzed CO_2 hydrogenation.[14b, 32]
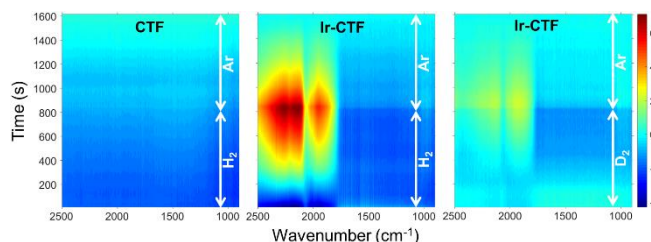
In summary, an iridium molecular complex ([IrCp*Cl₂]₂) is successfully immobilized on a solid covalent triazine framework. For the first time, catalytic activities of such a heterogenized catalyst are demonstrated under flow and even high pressure conditions in the presence/absence of a solvent/base. Some loss of weakly-bound Ir is detected, but the CTF provides sufficient binding strength to hold the Ir complex under harsh reaction conditions over some days of operation. This study also shows that methyl formate may serve as a practical intermediate for formic acid synthesis at higher reaction temperature where reaction kinetics are favored. The active roles of CTF through strong interaction with CO_2 are clarified, and so are the possible intermediates in CO_2 hydrogenation over the Ir-CTF. The present study opens new avenues for continuous formic acid synthesis over heterogenized catalysts, which may be inching closer to commercial viability.

Acknowledgements

Keywords: CO_2 hydrogenation • formic acid • heterogeneous catalysis • covalent triazine framework • continuous synthesis

[1] A. Álvarez, A. Bansode, A. Urakawa, A. V. Bavykina, T. A. Wezendonk, M. Makkee, J. Gascon, F. Kapteijn, *Chem. Rev.* **2017**, *117*, 9804-9838.
[2] aS. Enthaler, J. von Langermann, T. Schmidt, *Energ. Environ. Sci.* **2010**, *3*, 1207-1217; bH. Zhong, M. Iguchi, M. Chatterjee, Y. Himeda, Q. Xu, H. Kawanami, *Adv. Sustainable Syst.* **2018**, *2*, 1700161; cD. Mellmann, P. Sponholz, H. Junge, M. Beller, *Chem. Soc. Rev.* **2016**, *45*, 3954-3988.
[3] in *Ullmann's Encyclopedia of Industrial Chemistry*, **2011**.
[4] W.-H. Wang, Y. Himeda, in *Hydrogenation*, IntechOpen, **2012**.
[5] aN. Onishi, R. Kanega, E. Fujita, Y. Himeda, *Adv. Synth. Catal.* **2019**, *361*, 289-296; bS. Moret, P. J. Dyson, G. Laurenczy, *Nat. Commun.* **2014**, *5*, 4017; cR. Tanaka, M. Yamashita, K. Nozaki, *J. Am. Chem. Soc.* **2009**, *131*, 14168-14169; dJ. F. Hull, Y. Himeda, W.-H. Wang, B. Hashiguchi, R. Periana, D. J. Szalda, J. T. Muckerman, E. Fujita, *Nature Chemistry* **2012**, *4*, 383; eG. A. Filonenko, R. van Putten, E. N. Schulpen, E. J. M. Hensen, E. A. Pidko, *ChemCatChem* **2014**, *6*, 1526-1530; fJ. Fidalgo, M. Ruiz-Castañeda, G. García-Herbosa, A. Carbayo, F. A. Jalón, A. M.

Rodríguez, B. R. Manzano, G. Espino, *Inorg. Chem.* **2018**, *57*, 14186-14198.

[6] P. G. Jessop, F. Joó, C.-C. Tai, *Coordin. Chem. Rev.* **2004**, *248*, 2425-2442.

[7] M. Pérez-Fortes, J. C. Schöneberger, A. Boulamanti, G. Harrison, E. Tzimas, *Int. J. Hydrogen Energ.* **2016**, *41*, 16444-16462.

[8] aN. End, K.-U. Schöning, in *Immobilized Catalysts*, Springer, **2004**, pp. 241-271; bF. Cozzi, *Adv. Synth. Catal.* **2006**, *348*, 1367-1390.

[9] aC. Copéret, M. Chabanas, R. Petroff Saint-Arroman, J.-M. Basset, *Angew. Chem. Int. Edit.* **2003**, *42*, 156-181; bC. Copéret, F. Allouche, K. W. Chan, M. P. Conley, M. F. Delley, A. Fedorov, I. B. Moroz, V. Mougel, M. Pucino, K. Searles, K. Yamamoto, P. A. Zhizhko, *Angew. Chem. Int. Edit.* **2018**, *57*, 6398-6440.

[10] aS. Das, P. Heasman, T. Ben, S. Qiu, *Chem. Rev.* **2017**, *117*, 1515-1563; bP. Kaur, J. T. Hupp, S. T. Nguyen, *ACS Catal.* **2011**, *1*, 819-835; cJ. Artz, *ChemCatChem* **2018**, *10*, 1753-1771.

[11] aA. V. Bavykina, E. Rozhko, M. G. Goesten, T. Wezendonk, B. Seoane, F. Kapteijn, M. Makkee, J. Gascon, *ChemCatChem* **2016**, *8*, 2217-2221; bG. H. Gunasekar, K. Park, V. Ganesan, K. Lee, N.-K. Kim, K.-D. Jung, S. Yoon, *Chem. Mater.* **2017**, *29*, 6740-6748; cK. Park, G. H. Gunasekar , N. Prakash, K.-D. Jung, S. Yoon, *ChemSusChem* **2015**, *8*, 3410-3413.

[12] P. Katekomol, J. Roeser, M. Bojdys, J. Weber, A. Thomas, *Chemistry of Materials* **2013**, *25*, 1542-1548.

[13] S. Hug, M. E. Tauchert, S. Li, U. E. Pachmayr, B. V. Lotsch, *Journal of Materials Chemistry* **2012**, *22*, 13956-13964.

[14] aP. G. Jessop, Y. Hsiao, T. Ikariya, R. Noyori, *J. Am. Chem. Soc.* **1996**, *118*, 344-355; bA. Urakawa, F. Jutz, G. Laurenczy, A. Baiker, *Chem. Eur. J.* **2007**, *13*, 3886-3899.

[15] O. Buyukcakir, S. H. Je, S. N. Talapaneni, D. Kim, A. Coskun, *ACS Appl. Mater. Inter.* **2017**, *9*, 7209-7216.

[16] aG. Wang, K. Leus, S. Zhao, P. Van Der Voort, *ACS Appl. Mater. Inter.* **2018**, *10*, 1244-1249; bP. Kuhn, M. Antonietti, A. Thomas, *Angew. Chem. Int. Edit.* **2008**, *47*, 3450-3453; cR. Palkovits, M. Antonietti, P. Kuhn, A. Thomas, F. Schüth, *Angew. Chem. Int. Edit.* **2009**, *48*, 6909-6912; dR. Xu, X.-S. Wang, H. Zhao, H. Lin, Y.-B. Huang, R. Cao, *Catal. Sci. Technol.* **2018**, *8*, 2224-2230.

[17] G. H. Gunasekar, K. Park, H. Jeong, K.-D. Jung, K. Park, S. Yoon, *Catalysts* **2018**, *8*, 295.

[18] A. V. Bavykina, A. I. Olivos-Suarez, D. Osadchii, R. Valecha, R. Franz, M. Makkee, F. Kapteijn, J. Gascon, *ACS Appl. Mater. Inter.* **2017**, *9*, 26060-26065.

[19] A. V. Bavykina, M. G. Goesten, F. Kapteijn, M. Makkee, J. Gascon, *ChemSusChem* **2015**, *8*, 809-812.

[20] C. Mondelli, B. Puértolas, M. Ackermann, Z. Chen, J. Pérez-Ramírez, *ChemSusChem* **2018**, *11*, 2859-2869.

[21] aT. Arikawa, Y. Takasu, Y. Murakami, K. Asakura, Y. Iwasawa, *J. Phys. Chem. B* **1998**, *102*, 3736-3741; bW. Du, Q. Wang, D. Saxner, N. A. Deskins, D. Su, J. E. Krzanowski, A. I. Frenkel, X. Teng, *J. Am. Chem. Soc.* **2011**, *133*, 15172-15183.

[22] aM. Xiao, J. Zhu, G. Li, N. Li, S. Li, Z. P. Cano, L. Ma, P. Cui, P. Xu, G. Jiang, H. Jin, S. Wang, T. Wu, J. Lu, A. Yu, D. Su, Z. Chen, *Angew. Chem. Int. Edit.* **2019**, *58*, 9640-9645; bN. Tahir, F. Muniz-Miranda, J. Everaert, P. Tack, T. Heugebaert, K. Leus, L. Vincze, C. V. Stevens, V. Van Speybroeck, P. Van Der Voort, *J. Catal.* **2019**, *371*, 135-143.

[23] Y. A. Daza, J. N. Kuhn, *RSC Adv.* **2016**, *6*, 49675-49691.

[24] H. Park, J. H. Lee, E. H. Kim, K. Y. Kim, Y. H. Choi, D. H. Youn, J. S. Lee, *Chem. Commun.* **2016**, *52*, 14302-14305.

[25] H. Reymond, J. J. Corral-Pérez, A. Urakawa, P. Rudolf von Rohr, *React. Chem. Eng.* **2018**, *3*, 912-919.

[26] J. J. Corral-Pérez, A. Bansode, C. S. Praveen, A. Kokalj, H. Reymond, A. Comas-Vives, J. VandeVondele, C. Copéret, P. R. von Rohr, A. Urakawa, *J. Am. Chem. Soc.* **2018**, *140*, 13884-13891.

[27] K. D. Vogiatzis, A. Mavrandonakis, W. Klopper, G. E. Froudakis, *ChemPhysChem* **2009**, *10*, 374-383.

[28] A. Iskra, A. S. Gentleman, A. Kartouzian, M. J. Kent, A. P. Sharp, S. R. Mackenzie, *J. Phys. Chem. A* **2017**, *121*, 133-140.

[29] D. H. Gibson, *Coordin. Chem. Rev.* **1999**, *185-186*, 335-355.

[30] C. Preti, G. Tosi, *Z. Anorg. Allg. Chem.* **1977**, *432*, 259-263.

[31] J.-H. Choi, N. E. Schloerer, J. Berger, M. H. G. Prechtl, *Dalton T.* **2014**, *43*, 290-299.

[32] A. Urakawa, M. Iannuzzi, J. Hutter, A. Baiker, *Chem. Eur. J.* **2007**, *13*, 6828-6840.

COMMUNICATION

Hold it tight! A solid covalent triazine framework (CTF) is able to retain active molecular Ir catalyst under continuous high-pressure, supercritical conditions to produce formic acid and methyl formate via CO_2 hydrogenation. The unique roles of CTF and Ir in the activation of CO_2, H_2 and methanol were uncovered by *in situ* IR spectroscopy.

$CO_2 + H_2 + CH_3OH$ / H_2O / Et_3N

$HCOOCH_3$ / $HCOOH$

Juan José Corral-Pérez, Amelia Billings, Dragos Stoian, and Atsushi Urakawa*

Page No. – Page No.

Continuous hydrogenation of carbon dioxide to formic acid and methyl formate by a molecular iridium complex stably heterogenized on a covalent triazine framework